Inorg. Chem. **2004**, *43*, 4487–4495

Photolabile Ruthenium Nitrosyls with Planar Dicarboxamide Tetradentate N_4 Ligands: Effects of In-Plane and Axial Ligand Strength on NO Release

Apurba K. Patra,[†] Michael J. Rose,[†] Karen A. Murphy,[†] Marilyn M. Olmstead,[‡] and Pradip K. Mascharak*,[†]

Department of Chemistry and Biochemistry, University of California, Santa Cruz, California 95064, and Department of Chemistry, University of California, Davis, California 95616

Received February 25, 2004

Four ruthenium nitrosyls, namely [(bpb)Ru(NO)(Cl)] (**1**), [(Me_2bpb)Ru(NO)(Cl)] (**2**), [(Me_2bpb)Ru(NO)(py)](BF_4) (**3**), and [(Me_2bqb)Ru(NO)(Cl)] (**4**) (H_2bpb = 1,2-bis(pyridine-2-carboxamido)benzene, H_2Me_2bpb = 1,2-bis(pyridine-2-carboxamido)-4,5-dimethylbenzene, H_2Me_2bqb = 1,2-bis(quinaldine-2-carboxamido)-4,5-dimethylbenzene; H is the dissociable amide proton), have been synthesized and characterized by spectroscopy and X-ray diffraction analysis. All four complexes exhibit ν_{NO} in the range 1830–1870 cm^{-1} indicating the {Ru–NO}^{6} configuration. Clean ^{1}H NMR spectra in CD_3CN (or $(CD_3)_2SO$) confirm the $S = 0$ ground state for all four complexes. Although the complexes are thermally stable, they release NO upon illumination. Rapid NO dissociation occurs when solutions of **1**–**3** in acetonitrile (MeCN) or DMF are exposed to low-intensity (7 mW) UV light (λ_{max} = 302 nm). Electron paramagnetic resonance (EPR) spectra of the photolyzed solutions display anisotropic signals at $g \approx 2.00$ that confirm the formation of solvated low-spin Ru(III) species upon NO release. The ligand trans to bound NO namely, anionic Cl^- and neutral pyridine, has significant effect on the electronic and NO releasing properties of these complexes. Change in the in-plane ligand strength also has effects on the rate of NO release. The absorption maximum (λ_{max}) of **4** is significantly red shifted (455 nm in DMF) compared to the λ_{max} values of **1**–**3** (380–395 nm in DMF) due to the extension of conjugation on the in-plane ligand frame. As a consequence, **4** is also sensitive to visible light and release NO (albeit at a slower rate) upon illumination to low-intensity visible light (λ > 465 nm). Collectively, the photosensitivity of the present series of ruthenium nitrosyls demonstrates that the extent of NO release and their wavelength dependence can be modulated by changes of either the in-plane or the axial ligand (trans to bound NO) field strength.

Introduction

Nitric oxide (NO) plays important roles in a wide variety of physiological processes, including neurotransmission, immune response, blood pressure control, and inhibition of tumor growth.[1,2] As a consequence, compounds that deliver NO under controlled conditions are of great interest.[3] For example, NO donors that are capable of releasing NO upon illumination could find use as drugs in phototherapy. Indeed in recent years, intense effort has been directed toward metal nitrosyl complexes[4,5] that release NO upon illumination since such species could be used as antitumor agents in photodynamic therapy (PDT).[6] Although a vast number of metal nitrosyls are reported in the literature, very few of them release NO upon illumination. Metal porphyrins with NO as the fifth or sixth ligands do show NO photolability, and hence their photochemistry has been studied in detail.[4] However, NO release from these complexes is often beset with problems related to back-reaction (NO recombination). Several groups have utilized non-heme iron nitrosyls such

* Author to whom correspondence should be addressed. E-mail: pradip@chemistry.ucsc.edu.
[†] University of California at Santa Cruz.
[‡] University of California at Davis.

(1) (a) *Methods in Nitric Oxide Research*; Feelisch, M.; Stamler, J. S., Eds.; Wiley: Chichester, U.K., 1996. (b) Culotta, E.; Koshland, D. E. *Science*. **1992**, *258*, 1862−1865. (c) Feldman, P. L.; Griffith, O. W.; Stuehr, D. J. *Chem. Eng. News* **1993**, *71*, 26−31.
(2) (a) *Nitric Oxide: Biology and Pathobiology*; Ignaro, L. J., Ed.; Academic Press: San Diego, CA, 2000. (b) *Nitric Oxide and Infection*; Fang, F. C., Ed.; Kluwer Academic/Plenum: New York, 1999.

10.1021/ic040030t CCC: $27.50
Published on Web 06/09/2004

as sodium nitroprusside ($Na_2[Fe(CN)_5(NO)]$) and Roussin's salts ($(NH_4)[Fe_4S_3(NO)_7]$, $Na_2[Fe_2S_2(NO)_4]$) in their light-driven NO release studies.[3,5] These compounds do show some promise as photoactive NO donors.

Photolysis studies on ruthenium nitrosyls (congener of iron nitrosyls) have so far been quite limited. Franco and co-workers have shown that aqueous solutions of *trans*-$[Ru(NH_3)_4(NO)X]^{3+}$ release NO when irradiated in the 310−370 nm range and generate *trans*-$[Ru(NH_3)_4(H_2O)X]^{3+}$.[7] Light-induced NO release has also been observed with the non-porphyrin ruthenium nitrosyls [Ru(salen)(Cl)(NO)], $[Ru(salen)(NO)(H_2O)]^+$ (H_2salen = *N*,*N*′-bis(salicylaldehyde)-ethylenediimine), and related complexes.[8,9] In general, the ruthenium nitrosyls require high-energy UV light for NO release. The only exception is the very recently reported pyrazine-bridged diruthenium nitrosyl namely $[Ru(NH_3)_5(pz)Ru(bpy)_2(NO)]^{5+}$ that releases NO upon illumination in the visible range.[10]

As part of our work in the area of designed non-heme iron and other metal nitrosyls that release NO *upon mild irradiation*, we have recently reported that binding of NO at the non-heme Fe(III) center in $[(PaPy_3)Fe(MeCN)](ClO_4)_2$ ($PaPy_3H$ = *N*,*N*-bis(2-pyridylmethyl)amine-*N*-ethyl-2-pyridine-2-carboxamide, where H is the dissociable amide proton) is completely reversible.[11] This iron nitrosyl $[(PaPy_3)Fe(NO)](ClO_4)_2$ rapidly releases NO upon short exposure to low-intensity (50 W) visible light and is converted into the solvato species $[(PaPy_3)Fe(Solv)](ClO_4)_2$. Very recently, we have also reported the water-soluble photolabile ruthenium nitrosyl $[Ru(PaPy_3)(NO)](BF_4)_2$ that rapidly delivers NO to proteins such as reduced myoglobin and cytochrome *c* oxidase in aqueous solution upon short exposure to low-intensity UV light (7 mW/cm^2).[12] Our studies on these iron and ruthenium nitrosyl of $PaPy_3H$ ligand have shown that the negatively charged carboxamido N trans to the bound NO group triggers the release of NO.[11,12] To further establish the effects of the trans donor (trans to NO) and the in-plane ligand strength, we have now employed two tetradentate planar dicarboxamide N_4 ligands H_2bpb and its ring-substituted derivative H_2Me_2bpb (H_2bpb = 1,2-bis(pyridine-2-carboxamido)benzene and H_2Me_2bpb = 1,2-bis(pyridine-2-carboxamido)-4,5-dimethylbenzene, H's are the dissociable amide protons) in the synthesis of photoactive ruthenium nitrosyls. In this paper, we report the syntheses, structures, and spectral parameters of the ruthenium nitrosyls [(bpb)-Ru(NO)(Cl)] (**1**), [(Me_2bpb)Ru(NO)(Cl)] (**2**), and [(Me_2bpb)-Ru(NO)(Py)](BF_4) (**3**). The results of the kinetic studies on the photorelease of NO by these three ruthenium nitrosyls upon exposure to UV light of low intensity are also included. Comparison of the kinetic parameters clearly indicates that both increase the in-plane ligand strength (**1** and **2**) and change of the trans ligand (**2** and **3**) have significant effect on the rate of NO release from these nitrosyls. To probe whether the absorption maximum (λ_{max}) of this type of ruthenium complexes can be brought to the visible region, we have also synthesized and structurally characterized the complex [(Me_2bqb)Ru(NO)(Cl)] (**4**), where H_2Me_2bqb is 1,2-bis(quinaldine-2-carboxamido)-4,5-dimethylbenzene, a ligand with additional conjugation due to replacement of pyridine carboxylic acid with quinaldic acid. Herein we report that this photoactive nitrosyl with λ_{max} at 455 nm (red shifted compared to **1**−**3**) does release NO upon illumination with visible (λ > 465 nm) light.

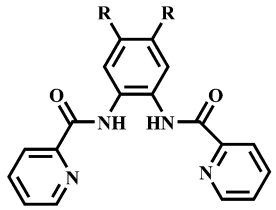

R = H, H_2bpb
R = Me, H_2Me_2bpb

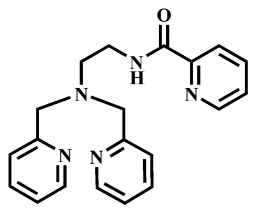

$PaPy_3H$

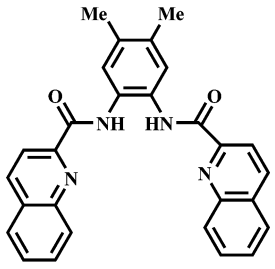

H_2Me_2bqb

Experimental Section

Materials and Reagents. 1,2-Diaminobenzene, 4,5-dimethyl-1,2-diaminobenzene, picolinic acid, quinaldic acid, and triphenyl phosphite were purchased from Aldrich Chemical Co. and used without further purification. NO gas was procured from Johnson Mathew Chemical Co. and was purified by passing through a long KOH column before use. $RuCl_3 \cdot xH_2O$ was purchased from Aldrich Chemical Co. and was treated several times with concentrated HCl to prepare the starting metal salt, $RuCl_3 \cdot 3H_2O$. All of the solvents were purified and/or dried by standard techniques and distilled prior

(3) (a) Wang, P. G.; Xian, M.; Tang, X.; Wu, X.; Wen, Z.; Cai, T.; Janczuk, A. *Chem. Rev.* **2002**, *102*, 1091−1134. (b) Hrabie, J. A.; Keefer, L. K. *Chem. Rev.* **2002**, *102*, 1135−1154. (c) Wang, K.; Zhang, W.; Xian, M.; Hou, Y.-C.; Chen, X.-C.; Cheng, J.-P.; Wang, P. G. *Curr. Med. Chem.* **2000**, *7*, 821−834. (d) Hou, Y.-C.; Janczuk, A.; Wang, P. G. *Curr. Pharm. Des.* **1999**, *5*, 417−441.
(4) (a) Ford, P. C.; Lorkovic, I. M. *Chem. Rev.* **2002**, *102*, 993−1017. (b) Bourassa, J. L.; Ford, P. C. *Coord. Chem. Rev.* **2000**, *200*, 887−900. (c) Hoshino, M.; Laverman, L.; Ford, P. C. *Coord. Chem. Rev.* **1999**, *187*, 75−102. (d) Ford, P. C.; Bourassa, J.; Miranda, K.; Lee, B.; Lorkovic, I.; Boggs, S.; Kudo, S.; Laverman, L. *Coord. Chem. Rev.* **1998**, *171*, 185−202.
(5) (a) Butler, A. R.; Megson, I. L. *Chem. Rev.* **2002**, *102*, 1155−1165. (b) Clarke, M. J.; Gaul, J. B. *Struct. Bonding* **1993**, *81*, 147−181.
(6) (a) Ackroyd, R.; Kelty, C.; Brown, N.; Reed, M. *Photochem. Photobiol.* **2001**, *74*, 656−669. (b) Pandey, R. K. *J. Porphyrins Phthalocyanines* **2000**, *4*, 368−373.
(7) (a) Tfouni, E.; Krieger, M.; McGarvey, B. R.; Franco, D. W. *Coord. Chem. Rev.* **2003**, *236*, 57−69. (b)Gomes, M. G.; Davanzo, C. U.; Silva, S. C.; Lopes, L. G. F.; Santos, P. S.; Franco, D. W. *J. Chem. Soc., Dalton Trans.* **1998**, 601−607.
(8) (a) Works, C. F.; Jocher, C. J.; Bart, G. D.; Bu, X.; Ford, P. C. *Inorg. Chem.* **2002**, *41*, 3728−3739. (b) Works, C. F.; Ford, P. C. *J. Am. Chem. Soc.* **2000**, *122*, 7592−7593.
(9) Bordini, J.; Hughes, D. L.; Da Motta Neto, J. D.; da Cunha, C. J. *Inorg. Chem.* **2002**, *41*, 5410−5416.
(10) Sauaia, M. G.; de Lima, R. G.; Tedesco, A. C.; da Silva, R. S. *J. Am. Chem. Soc.* **2003**, *125*, 14718−14719.
(11) Patra, A. K.; Afshar, R.; Olmstead, M. M.; Mascharak, P. K. *Angew. Chem., Int. Ed.* **2002**, *41*, 2512−2515.
(12) Patra, A. K.; Mascharak, P. K. *Inorg. Chem.* **2003**, *42*, 7363−7365.

to use. Standard Schlenk techniques were used during all syntheses to avoid exposure to dioxygen. Elemental analyses were performed by Prevalere Life Sciences, Inc.

Syntheses of Compounds. The ligands 1,2-bis(pyridine-2-carboxamido)benzene (H_2bpb) and 1,2-bis(pyridine-2-carboxamido)-4,5-dimethylbenzene (H_2Me_2bpb) was synthesized according to the literature procedure.[13]

1,2-Bis(quinoline-2-carboxamido)-4,5-dimethylbenzene (H_2Me_2bpb). A solution of 0.2 g (1.45 mmol) of 4,5-dimethyl-1,2-phenylenediamine in 2.5 mL of dry pyridine was slowly added to a solution of 0.5 g (2.89 mmol) of quinaldic acid in pyridine (2.5 mL). The reaction mixture was then placed on a water bath at 100 °C, and a batch of 0.9 g (2.89 mmol) of triphenyl phosphite was added dropwise with constant stirring. After additional stirring for 5 h at 100 °C, the clear solution was concentrated to half of its original volume and then stored at 0 °C. The desired product precipitated out as a white solid within 12 h. It was filtered out, washed with 30 mL of ethanol and 20 mL diethyl ether (Et_2O), and dried under vacuum (yield, 57%). ^{1}H NMR (500 MHz, CD_3Cl, δ from TMS): 2.27 (s, 6H, Me), 7.45 (m, 4H), 7.62 (s, 2H), 7.89 (m, 4H), 8.31 (d, 2H), 8.55 (m, 2H), 10.47 (s, 2H).

[(bpb)Ru(NO)(Cl)] (1). A slurry of 0.15 g (6.25 mmol) of NaH in 4 mL of DMF was added to a stirred solution of 1.0 g of H_2bpb (3.14 mmol) in 30 mL of dry DMF. The color of the solution turned clear yellow when the evolution of hydrogen gas stopped. A batch of 0.82 g (3.13 mmol) of solid $RuCl_3 \cdot 3H_2O$ was then added to this solution. The color of the mixture turned dark brown almost immediately. It was then heated to reflux for 20 h under dinitrogen. The dark green solution thus obtained was cooled to room temperature and filtered through a cintered glass crucible to remove NaCl. The filtrate was again heated to reflux and purified NO gas was allowed to pass through it for 3 h. The reaction mixture was then concentrated to 10 mL, and 10 mL of Et_2O was added. The dark brown compound that precipitated out was filtered off and washed with dry Et_2O and dried under vacuum (1.25 g, 82% yield). Crystals of [(bpb)Ru(NO)(Cl)] (**1**), suitable for X-ray diffraction, were grown via diffusion of Et_2O into a DMF solution of the complex. Anal. Calcd for $C_{18}H_{12}ClRuN_5O_3$ (**1**): C, 44.77; H, 2.50; N, 14.50. Found: C, 44.63; H, 2.48; N, 14.52. Selected IR frequencies (KBr disk, cm^{-1}): 1867 (ν_{NO}, vs), 1634 (vs), 1596 (s), 1472 (m), 1446 (w), 1375 (m), 1284 (w), 1093 (w), 756 (m). Electronic absorption spectrum in MeCN, λ_{max} (in nm) (ϵ in M^{-1} cm^{-1}): 380 (5960), 300 (9850), 275 (15 755). Electronic absorption spectrum in DMF, λ_{max} (in nm) (ϵ in M^{-1} cm^{-1}): 380 (5150), 300 (9350), 275 (15 110). ^{1}H NMR (500 MHz, $(CD_3)_2SO$, δ from TMS): 9.26 (d, 2H), 8.57 (m, 2H), 8.40 (t, 2H), 8.21 (d, 2H), 7.96 (t, 2H), 7.06 (m, 2H).

[(Me_2bpb)Ru(NO)(Cl)]·toluene (2·tol). This complex was synthesized by following the procedure described above. In this case, 1 g of H_2Me_2bpb, 0.14 g of NaH, and 0.75 g of $RuCl_3 \cdot 3H_2O$ were used in a total volume of 35 mL of dry DMF. NO was purged for 3 h, and after usual work up, a batch of 1.1 g of **2** was obtained (yield 75%). Crystals suitable for X-ray diffraction were grown via slow evaporation of a solution of the complex in CH_2Cl_2/toluene mixture. Anal. Calcd for $C_{27}H_{24}ClRuN_5O_3$ (**2**·tol): C, 53.77; H, 4.01; N, 11.61. Found: C, 53.85; H, 3.96; N, 11.59. Selected IR frequencies (KBr disk, cm^{-1}): 1833 (ν_{NO}, vs), 1634 (vs), 1597 (s), 1485 (m), 1371 (m), 1094 (w), 1005 (w), 890 (w), 756 (m), 681 (w). Electronic absorption spectrum in MeCN, λ_{max} (in nm) (ϵ in M^{-1} cm^{-1}): 395 (5300), 302 (8970), 278 (14 650). ^{1}H NMR (500 MHz, CD_3CN, δ from TMS): 8.94 (d, 2H), 8.41 (s, 2H), 8.29 (t, 2H), 8.25 (d, 2H), 7.81 (m, 2H), 2.33 (s, 6H).

[(Me_2bpb)Ru(NO)(py)](BF_4) (3). A solution of 0.05 g (0.257 mmol) of $AgBF_4$ in 5 mL of MeCN was added to a stirred solution of 0.1 g (0.196 mmol) of **2** in 25 mL of MeCN, and the reaction mixture was heated to reflux for 20 h. The precipitate of AgCl that separated during this period was then removed by filtration through a cintered glass crucible with a Celite pad on top. Next, a batch of 0.06 g of dry pyridine was added to the filtrate and the reaction mixture was heated to reflux for 4 h. Finally, the clear red-brown solution was concentrated to 5 mL. Diffusion of dry Et_2O into this solution afforded 0.95 g of **3** as dark brown microcystralline solid (yield 76%). Anal. Calcd for $C_{25}H_{21}RuN_6O_3BF_4$ (**3**): C, 46.82; H, 3.30; N, 13.10. Found: C, 46.78; H, 3.28; N, 13.05. Selected IR frequencies (KBr disk, cm^{-1}): 1869 (ν_{NO}, vs), 1644 (vs), 1600 (s), 1484 (m), 1356 (m), 1083 (s), 880 (w), 763 (m), 698 (w), 684 (w). Electronic absorption spectrum in MeCN, λ_{max} (in nm) (ϵ in M^{-1} cm^{-1}): 394 (7170), 300 (13 550), 276 (21 550). ^{1}H NMR (500 MHz, CD_3CN, δ from TMS): 9.20 (d, 2H), 8.48 (s, 2H), 8.30 (t, 2H), 8.13 (m, 4H), 7.95 (m, 2H), 7.84 (m, 1H), 7.31 (t, 2H), 2.35 (s, 6H).

[(Me_2bqb)Ru(NO)(Cl)]·DMF (4·DMF). This complex was synthesized by following the procedure described under the synthesis of **1**. Passage of NO for 3 h through a reaction mixture containing 1.0 g (2.39 mmol) of the ligand H_2Me_2bqb, 0.12 g (4.79 mmol) of NaH, and 0.63 g (2.39 mmol) of $RuCl_3 \cdot 3H_2O$ in a total of 40 mL of dry DMF followed by similar work up afforded 1.1 g of **4** (yield 79%). Anal. Calcd for $C_{31}H_{27}ClRuN_6O_4$ (**4**·DMF): C, 54.43; H, 3.98; N, 12.28. Found: C, 54.61; H, 3.78; N, 12.32. Selected IR frequencies (KBr disk, cm^{-1}): 1842 (ν_{NO}, vs), 1634 (vs), 1600 (s), 1514 (m), 1483 (m), 1373 (s), 1095 (w), 756 (s), 613 (w), 497 (w), 460 (w). Electronic absorption spectrum in DMF, λ_{max} (in nm) (ϵ in M^{-1} cm^{-1}): 455 (3 200), 308 (19 600). ^{1}H NMR (500 MHz, CD_3CN, δ from TMS): 2.27 (s, 6H, Me), 7.56 (t, 2H), 7.86 (t, 2H), 7.96 (t, 2H), 8.33 (d, 2H), 8.39 (d, 4H), 9.06 (d, 2H).

Physical Methods. Absorption spectra were recorded on a Cary 50 Varian spectrophotometer. A Perkin-Elmer 1600 FTIR spectrophotometer was employed to monitor the infrared spectra. X-band electron paramagnetic resonance (EPR) spectra were obtained with a Bruker ELEXSYS 500 spectrometer. ^{1}H NMR spectra were recorded at 298 K on a Varian 500 MHz spectrometer. The absorption spectra were monitored on a Cary 50 spectrophotometer in fast scan mode (spectra shown in Figure 6). Changes in the electronic absorption spectra due to loss of NO from **1**−**4** upon illumination were recorded as follows. The cuvette containing the MeCN (or DMF) solution of the complex was placed on top of a UV-transilluminator (UVP-TM-36, λ_{max} = 302 nm; intensity, 7 mW/cm^2), and the UV lamp was turned on for specific time periods. The distance between the lamp and the sample was 3 cm. The experiments with visible light (in case of **1** and **4**) were performed as follows. A 0.1 mM solution of the nitrosyl in DMF was taken in a glass cuvette and placed at a distance of 2.5 cm from a 100 W tungsten lamp. In two separate experiments, two UV filters that allow visible light of wavelengths above 410 and 465 nm, respectively, were placed between the lamp and the cuvette to ensure irradiation only with visible light above those wavelengths. The samples were illuminated for 15 min, and the temperature of the whole assembly was kept constant at 25 °C with the aid of a cooling fan. In case of **1**, the development of the absorption band at 650 nm was monitored to find out the formation of the solvent-bound product (following loss of NO) while, in the case of **4**, observations were made on the appearance of the 740 nm band to follow the NO loss. With known values of the extinction coefficients of these

(13) Barnes, D. J.; Chapman, R. L.; Vagg, R. S.; Watton, E. C. *J. Chem. Eng. Data* **1978**, *23*, 349−350.

bands for the corresponding solvent-bound species (obtained via exhaustive photolysis with UV light), the % loss values for the nitrosyls upon 15 min illumination were calculated.

Photolysis Experiments. Kinetic studies on the photolysis reactions were carried out with a Cary 50 Varian spectrophotometer. Solutions of **1**−**3** (~0.1×10^{-3} M) in MeCN were used. The cuvette was held at a fixed distance of 3 cm from the light source. Absorption spectra were taken after each irradiation for a certain period of time. Absorbance values at specific wavelengths (615 nm for **1**, 595 nm for **2**, and 570 nm for **3**) were obtained from the respective spectra, and observed rate constant values (K_{NO}) were obtained by fitting the absorbance values to the equation $A(t) = A_\infty + (A_0 - A_\infty)\{\exp(-K_{NO}t)\}$, where A_0 and A_∞ are respectively the initial and final absorbance values at the fixed wavelength. The rate constants shown are the mean value of three independent measurements in each case.

X-ray Data Collection and Structure Solution and Refinement. Diffraction data for **1**−**4** were collected either at 93 K (in case of **1**−**3**) or 186 K (in case of **4**) on a Bruker SMART 1000 system. Mo Kα (0.710 73 Å) radiation was used, and the data were corrected for absorption. The structures were solved by direct methods (standard SHELXS-97 package). In the structure of **2**·tol, the toluene molecule present as the solvent of crystallization is disordered with respect to rotation in the plane of the molecule. Part B was constrained to be the same as part A in the refinement; the relative occupancies refined to 0.587(8):0.413(8) for parts A and B, respectively. The atoms of the disordered toluene were kept isotropic in refinement. Crystals of **4**, suitable for diffraction, were grown via diffusion of Et_2O into solution of the complex in DMF. In the structure of **4**·DMF, the DMF molecule is also disordered over two sites. The occupancies were kept fixed in the refinement at 0.60:0.40 for the major (A atoms) and minor site (B atoms), respectively. The molecule was refined as a rigid group, but the thermal parameters were allowed to vary. All non-hydrogen atoms were refined with anisotropic displacement parameters, and hydrogen atoms were added geometrically and refined with the use of a riding model. Machine parameters, crystal data, and data collection parameters for all the complexes are summarized in Table 1 while selected bond distances and angles are listed in Table 2. Complete crystallographic data for [(bpb)Ru(NO)(Cl)] (**1**), [(Me_2bpb)Ru(NO)(Cl)]·toluene (**2**·tol), [(Me_2bpb)Ru(NO)(py)](BF_4) (**3**), and [(Me_2bqb)Ru(NO)(Cl)]·DMF (**4**·DMF) have been submitted as Supporting Information.

Table 1. Summary of Crystal Data and Intensity Collection and Structural Refinement Parameters for [(bpb)Ru(NO)(Cl)] (**1**), [(Me_2bpb)Ru(NO)(Cl)] (**2**·tol), [(Me_2bpb)Ru(NO)(Py)]BF_4 (**3**), and [(Me_2bqb)Ru(NO)(Cl)] (**4**·DMF)

	1	**2**	**3**	**4**
formula	$C_{18}H_{12}ClRuN_5O_3$	$C_{27}H_{24}ClRuN_5O_3$	$C_{25}H_{21}BF_4RuN_6O_3$	$C_{31}H_{27}ClRuN_6O_4$
mol wt	482.85	603.03	641.36	684.11
cryst color, habit	red needle	red-brown plate	red plate	black prism
T, K	93(2)	93(2)	90(2)	186(2)
cryst system	orthorhombic	monoclinic	triclinic	triclinic
space group	$P2_12_12_1$	$P2_1/c$	$P\bar{1}$	$P\bar{1}$
a, Å	10.2153(6)	10.0026(19)	8.894(2)	9.4257(7)
b, Å	12.3643(7)	30.898(6)	10.969(3)	12.8471(10)
c, Å	13.8577(9)	8.2255(16)	12.991(3)	12.8518(19)
α, deg	90	90	97.560(7)	114.395(2)
β, deg	90	99.930(4)	97.412(12)	90.090(2)
γ, deg	90	90	97.951(7)	91.813(3)
V, Å^3	1750.30(18)	2504.1(8)	1230.2(5)	1416.43(19)
Z	4	4	2	2
d_{calcd}, g cm^{-3}	1.832	1.600	1.731	1.604
abs coeff, μ, mm^{-1}	1.082	0.773	0.710	0.697
GOF[a] on F^2	1.052	1.103	1.078	1.076
R_1,[b] %	1.96	4.40	4.55	3.21
R_{w2},[c] %	5.07	9.20	11.48	7.86

[a] GOF = $[\sum w(F_o^2 - F_c^2)^2]/(M - N)]^{1/2}$ (M = number of reflections, N = number of parameters refined). [b] $R_1 = \sum||F_o| - |F_c||/\sum|F_o|$. [c] $R_{w2} = [\sum w(F_o^2 - F_c^2)^2]/\sum w(F_o)^2]]^{1/2}$.

Results and Discussion

Syntheses. The complexes **1**, **2**, and **4** were synthesized by following a general procedure. First, the ligand was deprotonated with NaH in dry DMF and then $RuCl_3 \cdot 3H_2O$ was allowed to react with the deprotonated ligand (bpb^{2-} or Me_2bpb^{2-}). Prolonged heating of this reaction mixture afforded a green solution and approximately 2 equiv of NaCl. This suggests that a [(bpb)Ru(DMF)(Cl)]-type of species is present in the green solution. Passage of NO through the hot solution of this intermediate afforded the desired complexes **1**, **2**, and **4** in ~80% yields after workup. Complex **3** was obtained from **2** by halide displacement reaction with $AgBF_4$ and subsequent reaction with pyridine in MeCN.

Structures of the Complexes. [(bpb)Ru(NO)(Cl)] (1). The molecular structure of **1** is shown in Figure 1, and selected bond distances and angles are listed in Table 2. The tetradentate ligand H_2bpb in its deprotonated form provides two neutral pyridine N and two anionic carboxamido N donors in the equatorial plane of the complex while the axial positions are occupied by NO and Cl^-. Thus, the geometry around the Ru(II) center is distorted octahedral. The average $Ru-N_{amide}$ distance (1.9901(14) Å) is considerably shorter than the average $Ru-N_{py}$ distance (2.1310(15) Å). The Ru−Cl distance (2.3683(4) Å) is comparable to the Ru−Cl distance of reported complexes with dianionic tetradentate (N_2O_2) ligands such as H_2salen, substituted H_2salophen, and H_2bpb derivatives.[8,9,14] The Ru−N(O) bond distance (1.7534(14) Å), N−O distance (1.1444(19) Å), and an almost linear Ru−N−O angle (172.37(14)°) of **1** are typical of $\{Ru-NO\}^6$ nitrosyls.[8−9,15] Multiple bond character between Ru and the NO moiety is indicated by the short Ru−N(O) bond.

[(Me_2bpb)Ru(NO)(Cl)]·toluene (2·tol). The overall structure of **2**, shown in Figure 2, is similar to that of **1**. The geometry around the Ru(II) center is distorted octahedral, and the bond distances and angles are comparable to those of **1** (Table 2). Both the average $Ru-N_{amide}$ and $Ru-N_{py}$ distances are slightly shorter than the corresponding distances

(14) Ko, P.-H.; Chen, T.-Y.; Zhu, J.; Cheng, K.-F.; Peng, S.-M.; Che, C.-M. *J. Chem. Soc., Dalton Trans.* **1995**, 2215−2219.

(15) (a) Lang, D. R.; Davis, J. A.; Lopes, L. G. F.; Ferro, A. A.; Vasconcellos, L. C. G.; Franco, D. W.; Tfouni, E.; Wieraszko, A.; Clarke, M. J. *Inorg. Chem.* **2000**, *39*, 2294−2300. (b) Bezerra, C. W. B.; Silva, S. C. d.; Gambardella, M. T. P.; Santos, R. H. A.; Plicas, L. M. A.; Tfouni, E.; Franco, D. W. *Inorg. Chem.* **1999**, *38*, 5660−5667. (c) Borges, S. d. S. S.; Davanzo, C. U.; Castellano, E. E.; Z-Schpector, J.; Silva, S. C.; Franco, D. W. *Inorg. Chem.* **1998**, *37*, 2670−2677. (d) Batista, A. A.; Pereira, C.; Wohnrath, K.; Queiroz, S. L.; Santos, R. H. de A.; Gamberdella, M. T. d. p. *Polyhedron* **1999**, *18*, 2079−2083. (e) Batista, A. A.; Pereira, C.; Queiroz, S. L.; Olveira, L. A. A. d.; Santos, R. H. de A.; Gamberdella, M. T. d. p. *Polyhedron* **1997**, *16*, 927−931. (f) Bohle, D. S.; Goodson, P. A.; Smith, B. D. *Polyhedron* **1996**, *15*, 3147−3150. (g) Ooyama, D.; Miura, Y.; Kitanaka, Y. K.; Howell, F. S.; Nagao, N.; Mukaida, M.; Nagao, H.; Tanaka, K. *Inorg. Chim. Acta* **1995**, *237*, 47−55.

Table 2. Selected Bond Distances (Å) and Angles (deg)

	Complex **1**		
Ru−N1	1.9904(15)	Ru−N2	1.9898(14)
Ru−N3	2.1299(15)	Ru−N4	2.1322(15)
Ru−N5	1.7534(14)	Ru−Cl1	2.3683(4)
N5−O3	1.1444(19)	C7−O1	1.230(2)
C13−O2	1.235(2)		
N1−Ru−N2	83.31(6)	N1−Ru−N3	80.19(6)
N1−Ru−N4	162.19(6)	N1−Ru−N5	96.76(6)
N1−Ru−Cl1	87.04(4)	N2−Ru−N3	162.26(6)
N2−Ru−N4	80.34(6)	N2−Ru−N5	98.83(6)
N2−Ru−Cl1	87.06(4)	N3−Ru−N4	115.04(6)
N3−Ru−N5	89.58(6)	N3−Ru−Cl1	85.63(4)
N4−Ru−N5	92.69(6)	N4−Ru−Cl1	85.12(4)
N5−Ru−Cl1	173.30(5)	Ru−N5−O3	172.37(14)
	Complex **2**		
Ru−N1	1.992(3)	Ru−N2	1.984(3)
Ru−N3	2.121(3)	Ru−N4	2.122(3)
Ru−N5	1.742(3)	Ru−Cl1	2.3718(9)
N5−O3	1.154(4)	C7−O1	1.233(4)
C13−O2	1.230(4)		
N1−Ru−N2	84.14(12)	N1−Ru−N3	79.72(12)
N1−Ru−N4	163.06(12)	N1−Ru−N5	97.95(12)
N1−Ru−Cl1	88.97(8)	N2−Ru−N3	161.90(11)
N2−Ru−N4	80.08(11)	N2−Ru−N5	97.01(13)
N2−Ru−Cl1	86.75(9)	N3−Ru−N4	114.84(11)
N3−Ru−N5	93.31(12)	N3−Ru−Cl1	84.83(8)
N4−Ru−N5	90.08(12)	N4−Ru−Cl1	84.06(8)
N5−Ru−Cl1	172.41(9)	Ru−N5−O3	173.90(3)
	Complex **3**		
Ru−N1	1.994(2)	Ru−N2	1.983(2)
Ru−N3	2.146(2)	Ru−N4	2.130(3)
Ru−N5	2.139(2)	Ru−N6	1.758(2)
N6−O3	1.147(3)	C7−O1	1.219(4)
C13−O2	1.224(3)		
N1−Ru−N2	82.28(10)	N1−Ru−N3	79.70(10)
N1−Ru−N4	159.84(10)	N1−Ru−N5	88.19(10)
N1−Ru−N6	95.21(11)	N2−Ru−N3	160.85(10)
N2−Ru−N4	79.93(10)	N2−Ru−N5	89.12(9)
N2−Ru−N6	100.56(10)	N3−Ru−N4	116.52(10)
N3−Ru−N5	83.90(9)	N3−Ru−N6	87.53(10)
N4−Ru−N5	82.16(9)	N4−Ru−N6	97.29(10)
N5−Ru−N6	170.08(10)	Ru−N6−O3	170.0(2)
	Complex **4**		
Ru−N1	1.9941(17)	Ru−N2	1.9936(17)
Ru−N3	2.1611(17)	Ru−N4	2.1859(18)
Ru−N5	1.7389(19)	Ru−Cl1	2.3627(6)
N5−O3	1.146(3)	C7−O1	1.231(2)
C17−O2	1.232(3)		
N1−Ru−N2	83.43(7)	N1−Ru−N3	78.58(7)
N1−Ru−N4	162.16(7)	N1−Ru−N5	94.21(8)
N1−Ru−Cl1	89.81(5)	N2−Ru−N3	159.49(7)
N2−Ru−N4	78.82(7)	N2−Ru−N5	96.88(8)
N2−Ru−Cl1	86.05(6)	N3−Ru−N4	118.53(6)
N3−Ru−N5	94.18(7)	N3−Ru−Cl1	84.15(5)
N4−Ru−N5	89.72(8)	N4−Ru−Cl1	87.19(5)
N5−Ru−Cl1	175.26(6)	Ru−N5−O3	177.77(19)

of **1**. This confirms the fact that the in-plane donor strength of Me_2bpb^{2-} is greater than that of the bpb^{2-} ligand. Mukherjee and co-workers have recently reported that alkyl substitution on the periphery of H_2bpb ligand increases the in-plane ligand field strength.[16] It is interesting to note that the Ru−Cl bond (2.3718(9) Å) of **2** is slightly longer than that in **1** while the Ru−N(O) bond (1.742(3) Å) is slightly

(16) Patra, A. K.; Ray, M.; Mukherjee, R. *Inorg. Chem.* **2000**, *39*, 652−657.

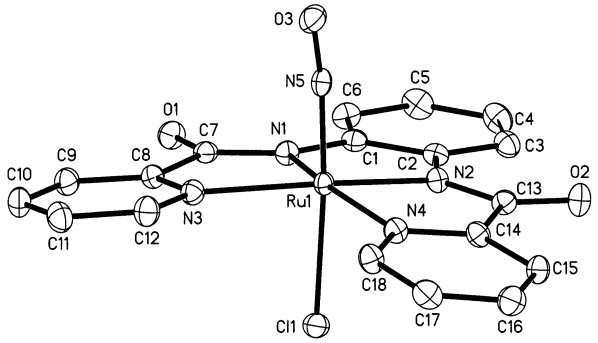

Figure 1. Thermal ellipsoid (probability level 50%) plot of [(bpb)Ru(NO)(Cl)] (**1**) with the atom-labeling scheme. H atoms are omitted for the sake of clarity.

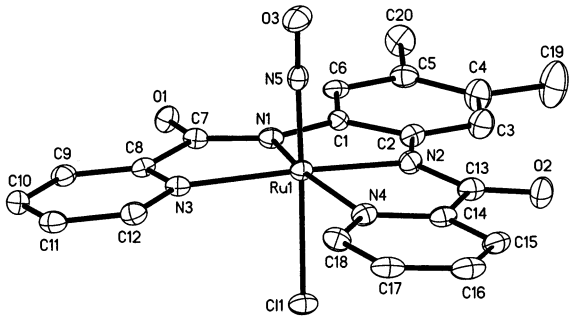

Figure 2. Thermal ellipsoid (probability level 50%) plot of [(Me_2bpb)Ru(NO)(Cl)] (**2**) with the atom-labeling scheme. H atoms are omitted for the sake of clarity.

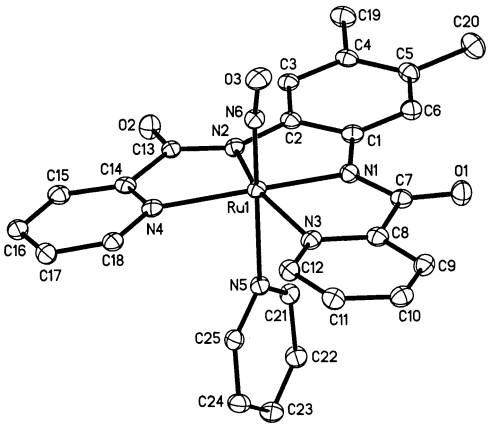

Figure 3. Thermal ellipsoid (probability level 50%) plot of [(Me_2bpb)Ru(NO)(py)]$^+$ (**3**) with the atom-labeling scheme. H atoms are omitted for the sake of clarity.

shorter (in **1** it is 1.7534(14) Å). The increased in-plane ligand strength thus appears to push electron density to NO via the ruthenium center. This is further supported by the fact that the N−O distance (1.154(4) Å) of **2** is slightly longer than the N−O distance of **1** (1.1444(19) Å).

[(Me_2bpb)Ru(NO)(py)](BF_4) (3). The structure of [(Me_2bpb)Ru(NO)(py)]$^+$, the cation of **3**, is shown in Figure 3 while the selected bond distances and angles are listed in Table 2. The four N atoms of the Me_2bpb^{2-} ligand are bonded to the Ru(II) center in the equatorial plane while the pyridine N and NO occupy the axial positions. Although the metric parameters related to the Me_2bpb^{2-} ligand in **3** are very similar to those observed in **2**, the Ru−N(O) distance (1.758(2) Å) of **3** is ∼0.02 Å longer than that of **2**. This

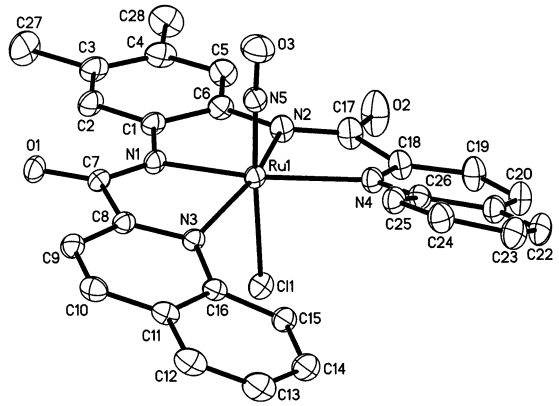

Figure 4. Thermal ellipsoid (probability level 50%) plot of [(Me_2bqb)-Ru(NO)(Cl)] (**4**) with the atom-labeling scheme. H atoms are omitted for the sake of clarity.

difference presumably arises from the different trans effect of the two ligands, namely, pyridine and Cl^-. Interestingly, the average C−O distance in **3** (1.221(4) Å) is slightly shorter than that of **1** (1.232(2) Å) and **2** (1.231(5) Å).

[(Me_2bqb)Ru(NO)(Cl)]·DMF (4·DMF). The structure of **4**, shown in Figure 4, is similar to that of **2** (Figure 2) with some minor differences. First of all, the in-plane ligand in **4** is more extended and is held with a twist. The dihedral angle between the two quinaldic acid portions is 25.2°. Strong steric interactions among the H atoms of the quinaldic acid moieties are the major reasons for this twist. For example, the H atoms on C15 and C25 would hit each other if the Me_2bqb^{2-} ligand were strictly planar. A drawing of the whole Me_2bqb^{2-} ligand with some displacements from the least-squares plane is shown in Figure S1 (Supporting Information). Also, both the average $Ru-N_{qu}$ (N_{qu} = quinoline N) and $Ru-N_{amide}$ distances of **4** are slightly longer than the corresponding distances noted for **2** (Table 2). And finally, the Ru−N−O angle (177.77(19)°) is greater than that of **2** (173.90(3)°). In fact, **4** exhibits the most linear Ru−N−O bonding among the four ruthenium nitrosyls reported in this paper (Table 2). A close scrutiny of Table 2 reveals that the Ru−N(O) distance and the Ru−N−O angle are correlated very well in the present set of ruthenium nitrosyls **1**−**4**. For example, **3** with the longest Ru−N(O) bond (1.758(2) Å) has the most bent Ru−N−O angle (170.0(2)°) while **4** with the shortest Ru−N(O) bond (1.7389(19) Å) exhibits the largest Ru−N−O angle (177.77(19)°). The correlation is even more apparent when one considers the three complexes **1**, **2**, and **4** with identical axial ligations. As the Ru−N(O) bond distances decrease from **1** (1.7534(14) Å) to **2** (1.742(3) Å) to **4** (1.7389(19) Å), the corresponding Ru−N−O angles increase from 172.37(14) to 173.90(3) to 177.77(19)°.

Spectroscopic Properties. All four complexes display strong carbonyl stretching frequencies (ν_{CO}) in the range 1630−1645 cm^{-1} which are red shifted compared to the ν_{CO} values of the free ligands (for H_2bpb, ν_{CO} = 1677 cm^{-1}, for H_2Me_2bpb, ν_{CO} =1666 cm^{-1}, and for H_2Me_2bqb, ν_{CO} =1689 cm^{-1}). This confirms coordination of the ligands in their deprotonated forms in these complexes.[17] The ν_{CO} values also

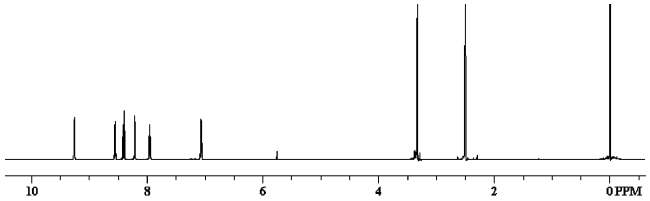

Figure 5. ^{1}H NMR spectrum (500 MHz) of **1** in $(CD_3)_2SO$ at 298 K. The two peaks at 2.5 and 3.3 ppm are due to DMSO and water.

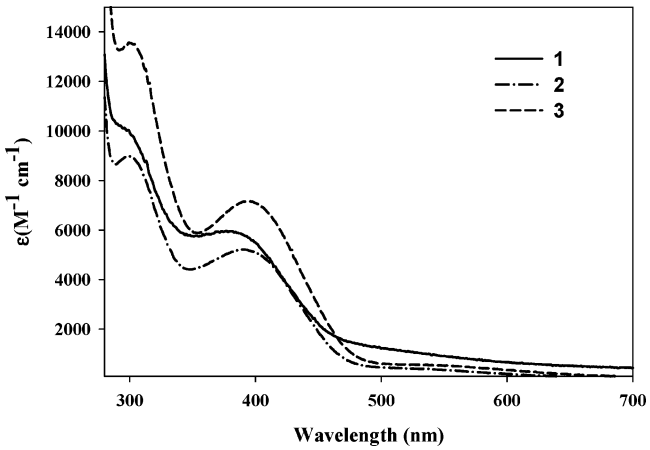

Figure 6. Electronic absorption spectra of **1**−**3** in MeCN.

correlate with the C−O distances noted with **1**−**4**. For example, both **1**, **2**, and **4** have practically identical C−O distances (∼1.23 Å) while it is slightly shorter in case of **3** (∼1.22 Å). Accordingly, **1**, **2**, and **4** exhibit ν_{CO} at 1634 cm^{-1} while **3** displays the same band at 1644 cm^{-1}. A single strong N−O stretching band (ν_{NO}) is observed for each of the four complexes. The ν_{NO} values, 1867, 1833, 1869, and 1842 cm^{-1}, respectively, for **1**−**4**, fall in the range expected for {Ru−NO}^{6} type complexes.[8,9] As discussed above in the structure section, stronger in-plane ligand field strength increases the N−O bond length (lesser NO^+ character) in **2** compared to **1**. This is nicely supported by the ν_{NO} values. The N−O stretching frequency drops from 1867 cm^{-1} (value for **1**) to 1833 cm^{-1} in case of **2**. Complexes **1** and **3** however exhibit practically the same ν_{NO} value (1867, 1869 cm^{-1}, respectively) since the N−O distances are identical in these two nitrosyls. Along the same line, the in-plane ligand strength of Me_2bqb^{2-} in **4** is somewhat weaker (Ru−N bonds longer) than that of Me_2bpb^{2-} in **2** and the ν_{NO} value of **4** (1842 cm^{-1}) is shifted to a slightly higher energy compared to **2** (1833 cm^{-1}). The ^{1}H NMR spectra of the complexes clearly indicate their $S = 0$ ground state. One representative ^{1}H NMR spectrum (the spectrum of **1**) is shown in Figure 5.

The electronic spectra of **1**−**3** in MeCN are displayed in Figure 6. All three complexes exhibit one strong intraligand absorption band with λ_{max} at ∼300 nm.[18] In addition, complex **1** displays a strong absorption with λ_{max} at 380 nm while, in the case of **2** and **3**, this band appears at 395 nm (Figure 6). The high extinction coefficient of this absorption band suggests a charge-transfer origin. Similar absorption bands

(17) Marlin, D. S.; Mascharak, P. K. *Chem. Soc. Rev.* **2000**, *29*, 69−74.

(18) Ray, M.; Mukherjee, R. N.; Richardson, J. F.; Buchanon, R. M. *J. Chem. Soc., Dalton Trans.* **1993**, 2451−2457.

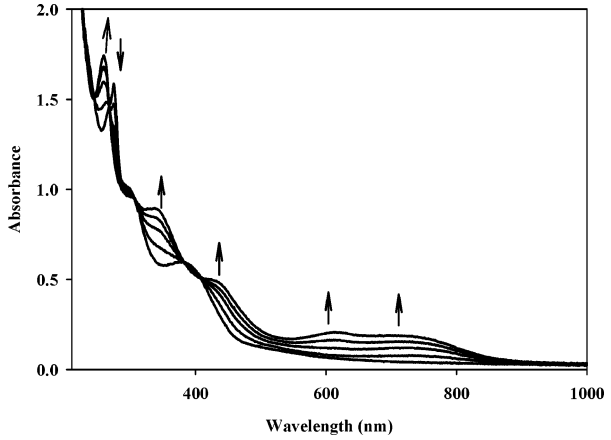

Figure 7. Conversion of [(bpb)Ru(NO)(Cl)] (**1**) into [(bpb)Ru(MeCN)-(Cl)] in MeCN solution upon illumination with a low-intensity UV lamp.

have been noted with [Ru(salen)(Cl)(NO)] and [Ru(^{t}Bu$_4$-salen)(Cl)(NO)] which have been assigned as d_π(Ru) $\rightarrow \pi^*$-(NO) metal-to-ligand charge transfer (MLCT) bands.[8] In case of the nitrosyls **1**−**3**, the ∼390 nm band most possibly arises from a similar MLCT transition. Red shift of the 380 nm band of **1** to 395 nm in the case of **2** and **3** indicates that the greater donor strength of the Me_2bpb^{2-} facilitates transfer of electron density from the metal to the π^* orbital of NO.

Photochemistry of 1−3. When solutions of the complexes **1**−**3** in MeCN are exposed to UV light, the resulting optical spectral changes are consistent with substitution of bound NO by MeCN molecule (eq 1).[12] Spectral changes upon irradiation of a ∼0.1 mM solution of **1** in MeCN with a low-intensity UV lamp (7 mW/cm^2, λ_{max} = 302 nm) are shown in Figure 7. Similar spectral changes have been observed with complexes **2** and **3** (Supporting Information, Figure S1 and S2). The clean conversion of the NO-bound ruthenium complex to the corresponding solvato species is indicated by the isosbestic points at 245, 266, 306, 382, and 409 nm (Figure 7). The [(bpb)Ru(MeCN)(Cl)] photoproduct exhibits increased absorbance at 257 and 339 nm while the new bands arise at ∼615 and ∼730 nm. It is important to note that no back-reaction is observed when the light is turned off. It thus appears that, in dilute solution, the solvent-bound species resists re-formation of the nitrosyl complex. All the photoproducts display a broad low-energy band in the range 700−900 nm which arises from bpb^{2-} to Ru(III) charge transfer (LMCT) transition.[14] Similar low-energy LMCT bands have been observed in the photoproducts of Ru nitrosyls derived from H_2salen and H_2salophen.[8,9]

$$[(L)Ru(NO)(X)] + MeCN \xrightarrow{h\nu} [(L)Ru(MeCN)(X)] + NO \quad (1)$$

$$L = bpb^{2-}, Me_2bpb^{2-}; X = Cl^-, py$$

A pseudo-first-order behavior has been observed in the photolysis of the present nitrosyls in coordinating solvents such as MeCN and DMF (Figure 8). The results of the study on photolysis of the solutions of **1**−**3** in MeCN are reported in this section (**4** is sparingly soluble in MeCN). The NO dissociation rates (K_{NO}) of **1**−**3** are 1.225 ± 0.002, 1.370 ± 0.003, and 0.431 ± 0.002 × 10^{-2} s^{-1}, respectively. It is important to note that the K_{NO} value of **2** is slightly higher than that of **1** but is significantly greater than that of **3**.

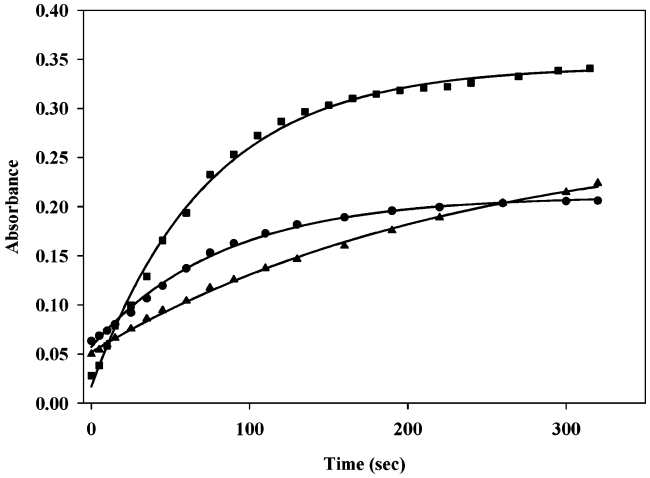

Figure 8. Increase in absorbance at ∼600 nm of a solution of **1** (circle), **2** (square), and **3** (triangle) in MeCN with time upon illumination with UV lamp.

The superior in-plane donor strength of Me_2bpb^{2-} therefore increases the axial NO releasing rate to a limited extent while a change in the trans ligand from neutral pyridine to Cl^- increases it considerably.[19] The greater effect of the trans ligand and in particular its negative charge on the overall photolability of NO in this class of metal nitrosyls are particularly noteworthy. We have previously commented on this effect while describing the photorelease of NO from [(PaPy$_3$)Fe(NO)](ClO$_4$)$_2$ and [Ru(PaPy$_3$)(NO)](BF$_4$)$_2$.[11,12]

EPR Analysis of the Photoproducts. To identify the oxidation state of ruthenium in the solvato species generated after complete photolysis of the diamagnetic ruthenium nitrosyls **1**−**3**, EPR measurements were performed on the photoproduct at 120 K. In general, Ru(III) (electronic configuration: $4d^5$) forms low-spin complexes, and in most cases, their EPR spectra do not exhibit hyperfine or superhyperfine couplings.[20−22] The EPR spectra of the photoproducts of **1** and **3** are shown in Figure 9. Photoproducts of **1** and **2** in DMF/toluene glass display rhombic EPR spectrum (*g* values: 2.46, 2.23, and 1.80 for **1** and 2.32, 2.22, and 1.85 for **2**) while the photoproduct of **3** exhibits an axial spectrum with *g* values at 2.17 and 1.88. The presence of two neutral N donors (MeCN and py) in [(Me$_2$bpb)Ru-(MeCN)(py)]$^+$ (photoproduct of **3**) presumably gives rise to the axial EPR spectrum (Figure 9, bottom panel). Similar EPR active species have been generated from the photolysis of [Ru(salen)(Cl)(NO)] and [Ru(salen)(H$_2$O)(NO)]$^+$ in different solvent medium.[9]

(19) Complexes **1** and **2** exhibit quasireversible cyclic voltammograms with $E_{1/2}$ = −0.44 and −0.46 V (vs SCE), respectively. Since the potential for $Ru^{III}-Ru^{II}$ couple in case of **2** is ∼20 mV more cathodic than that of **1**, it appears that the change in ligand filed strength is not very significant as one replaces bpb^{2-} with Me_2bpb^{2-}. This explains the slight change in the K_{NO} values noted with **1** and **2**.

(20) Ikezawa, H.; Miki, E.; Mizumachi, K.; Ishimori, T.; Nagai, T.; Tanaka, M. *Bull. Chem. Soc. Jpn.* **1993**, *66*, 89−97.
(21) Fairy, M. B.; Irving, R. J.; *J. Chem. Soc. A* **1966**, 475−479.
(22) Pandey, K. K.; Garg, K. H. *Polyhedron* **1995**, *14*, 1987−1991.

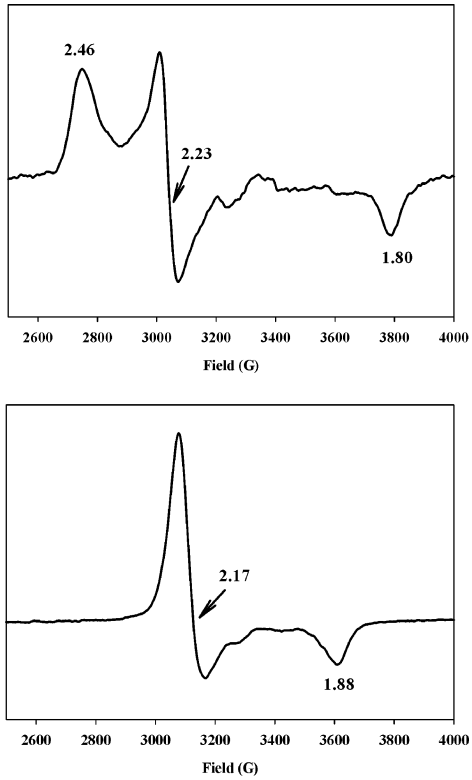

Figure 9. X-band EPR spectrum of the photoirradiated solutions of **1** (top) in DMF/toluene and **3** (bottom) in MeCN/toluene at 120 K. Spectrometer settings: microwave power, 50 mW; microwave frequency, 9.49 GHz; modulation frequency, 100 kHz; modulation amplitude, 2 G.

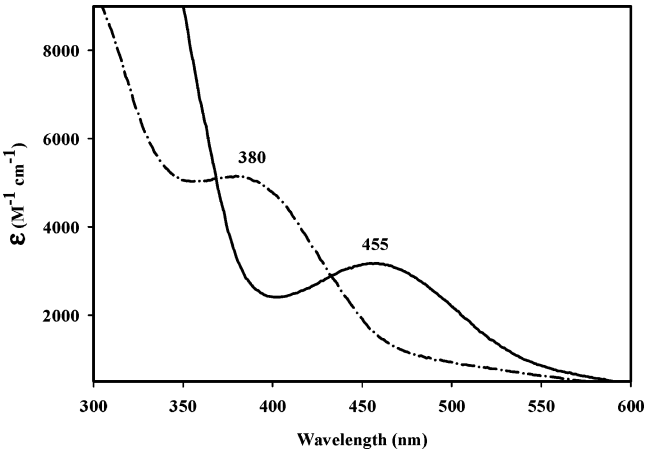

Figure 10. Absorption spectra of **1** (broken line) and **4** (solid line) in DMF.

Photochemistry of 4: Shift of λ_{max} via Ligand Manipulation. Since NO donors that release NO upon illumination in the visible range are often preferred as potential candidates for drug use, we have explored the possibility of NO release from **4** upon exposure to visible light. The use of a more conjugated ligand Me_2bqb^{2-} shifts the λ_{max} of this nitrosyl to the visible region. For example, in DMF, **4** exhibits its λ_{max} at 455 nm while **1** displays its λ_{max} at 380 nm (Figure 10). It is therefore evident that alteration of the in-plane ligand does shift the λ_{max} of this type of nitrosyls and extended conjugation brings about a red shift of the λ_{max} value. Much like **1**−**3**, complex **4** rapidly releases NO (K_{NO} = (1.285 ± 0.004) × 10^{-2} s^{-1} in DMF) when exposed to the same low-intensity UV illumination (7 mW/cm^2, λ_{max} = 302 nm). To test whether **4** has any sensitivity toward visible light, solutions of **4** in DMF were illuminated with light of wavelengths (λ) above 410 and 465 nm for 15 min in two different experiments. Significant extent of NO loss (20%) was observed in case of visible lights with λ > 410 nm while light with λ > 465 nm resulted in 16% loss of NO from **4**. Since control experiments with **1** afforded 14% (with λ > 410 nm) and 1% (with λ > 465 nm) NO loss, it appears that **4** is more sensitive to visible light compared to **1**. Collectively, these results indicate that the absorption maxima of this kind of nitrosyls could be brought to the visible range by altering the in-plane ligand frame with additional conjugation and the resulting nitrosyls (such as **4**) could release NO upon exposure to visible light. Since the strong UV absorption band(s) of **4** arising from the organic moieties has considerable overlap with the 455 nm band (Figure 10), we could not clearly demonstrate the effect of visible light on NO loss by this designed nitrosyl. At present, we are trying to modify the ligand frame such that the resulting complex exhibits its visible absorption band well separated from the strong UV band(s). We anticipate that such a nitrosyl will release NO exclusively upon exposure to visible light.[10]

Summary and Conclusions

The following are the principal findings and conclusions of this investigation:

(1) A series of photolabile ruthenium nitrosyls of $\{Ru-NO\}^6$ type (**1**−**4**) have been synthesized by using three tetradentate dicarboxamide N_4 ligands (H_2bpb, H_2Me_2bpb, and H_2Me_2bqb). The planar dianionic ligands are coordinated in the basal plane of these complexes. In **1**, **2**, and **4**, a chloride ion is trans to the bound NO while, in **3**, NO is trans to a neutral pyridine ligand.

(2) All four ruthenium nitrosyls are photoactive and rapidly lose NO upon exposure to low-intensity UV light. The EPR spectra of the photoproducts of the formally Ru(II) nitrosyls confirm the formation of the corresponding $[(L)Ru^{III}(L')(Sol)]^+$ (L = tetradentate ligand; L′ = Cl^- or py) species upon the release of NO.

(3) The rates of NO loss from **1**−**3** upon illumination (K_{NO}) in MeCN indicate that the ligand trans to bound NO has considerable influence on the NO photolability. Increase in the in-plane ligand field strength brings about red shifts of the absorption maximum (λ_{max}) and the N−O stretching frequency (ν_{NO}) in these nitrosyls.

(4) Addition of phenyl rings (more extended conjugation) to the ligand frame in case of **4** makes this nitrosyl more sensitive to visible light (with λ > 465 nm). It thus appears that the λ_{max} values of this kind of nitrosyls could be red shifted via alterations in the in-plane ligand frame. Such modifications could afford nitrosyls that release NO exclusively upon illumination with visible light.

Acknowledgment. Financial support from a NIH grant (GM 61636) is gratefully acknowledged. The Bruker SMART 1000 diffractometer was funded in part by the NSF Instrumentation Grant CHE-9808259.

Supporting Information Available: A drawing of the whole Me_2bqb^{2-} ligand with some displacements from the least-squares plane (Figure S1), absorption spectral changes of **2** and **3** in MeCN upon illumination with UV light (Figure S2 and Figure S3), increase in absorbance at 566 nm of a solution of **4** in DMF with time upon illumination with UV lamp (Figure S4), and X-ray crystallographic data (in CIF format) and tables for the structure determination of complexes [(bpb)Ru(NO)(Cl)] (**1**), [(Me_2bpb)Ru(NO)(Cl)] (**2**·tol), [(Me_2bpb)Ru(NO)(py)] (**3**), and [(Me_2bqb)Ru(NO)(Cl)]·DMF (**4**·DMF). This material is available free of charge via the Internet at http://pubs.acs.org.

IC040030T